Original Research

Precise 3D Skeletal Kinematics Using Fast Phase Contrast Magnetic Resonance Imaging

Andrea J. Rebmann, MBE,[2,3] and Frances T. Sheehan, PhD[1,3,4]*

Purpose: To examine the precision of cine-phase contrast (PC) magnetic resonance imaging (MRI) techniques as applied to the quantification of three-dimensional knee joint kinematics.

Materials and Methods: The knee joints of eight healthy volunteers were studied using three different dynamic, PC MRI protocols: cine-PC (one average), cine-PC (two averages), and cine-PC with segmented phase encoding (fast-PC).

Results: Fast-PC has comparable precision, shorter scan times, and improved subject interexam variability (SIEV) compared to cine-PC (two averages). Further, cine-PC (one average) has low precision and high SIEV, making fast-PC the preferred method of data acquisition. Specifically, the precision of fast-PC MRI in measuring knee joint kinematics ranged from 0.22°–1.16°.

Conclusion: A cine-PC MRI technique utilizing segmented phase encoding (fast-PC MRI) acquires dynamic data at a faster rate than other PC imaging protocols, without compromising data precision. Being able to acquire precise 3D kinematics with shorter imaging times is critical if we are to use this technique to advance ongoing research in musculoskeletal kinematics.

Key Words: musculoskeletal; dynamic MRI; patella; femur; tibia; knee
J. Magn. Reson. Imaging 2003;17:206–213.

NONINVASIVELY QUANTIFYING IN VIVO three-dimensional (3D) musculoskeletal dynamics is critical if we are to understand the etiology of musculoskeletal impairments and improve the diagnosis and treatments of such impairments (1). Cine phase contrast magnetic resonance imaging (cine-PC MRI) has been shown to be accurate in acquiring such measures (2,3). Obviously, the viability of any measurement technique is founded upon both its accuracy and precision. Thus, the purpose of this study was to define the precision of cine-PC MRI and determine if a new, faster technique, utilizing segmented phase encoding (fast-PC MRI), can be used to acquire the same measures with equal or better precision in less time.

Although skeletal kinematics have been studied extensively, there are still many unresolved questions regarding the relationship between impairments (altered joint dynamics) and specific physical disabilities, due to the variability in results and methods across studies (4). For example, in studying knee joint kinematics, much variability arises from the range of experimental tools used to study this joint (e.g., ultrasound, x-ray, computed tomography (CT), MRI, gait analysis, and invasive procedures). In addition, few studies have investigated the complete knee joint (patello-tibio-femoral joint), opting to study the patellofemoral or the tibiofemoral joint in isolation. Lastly, these joints have been studied under static (5–7), quasi-static (8–10), or dynamic (11–17) conditions; in two and three dimensions; in healthy subjects, in patients with specific impairments and using cadavers. Such variety in experimental protocols leads to confusion when trying to establish baseline levels for healthy and impaired joint function. Also, numerous studies are based on qualitative measures only (18), making cross-study comparisons nearly impossible.

The long-term goal of our research is to develop and test a set of clinical tools, virtual functional anatomy (VFA), for the precise and accurate quantification of 3D musculoskeletal kinematics. We envision VFA being integrated with long standing clinical evaluation tools in order to improve the diagnosis and treatment of various musculoskeletal impairments. For example, in the arena of surgical intervention, such a quantitative tool will not only help in surgical planning (19), but also support the growing interest in robotic surgery. A key aspect of VFA is that the skeletal kinematics are derived by integrating the PC velocity data (16,20). Thus, quantifying complete 3D kinematics and defining clinical

[1]Mechanical Engineering, Catholic University of America, Washington, DC.
[2]Biomedical Engineering, Catholic University of America, Washington, DC.
[3]National Institutes of Health Diagnostic Radiology Department, Bethesda, Maryland.
[4]National Institutes of Health Physical Disabilities Branch, Bethesda, Maryland.
Presented at ISMRM, Glasgow, Scotland, 2001.
The opinions presented in this report reflect the views of the authors and not those of the National Institutes of Health, the U.S. Public Health Service, or the Catholic University of America.
*Address reprint requests to: F.T.S., Mechanical Engineering, Catholic University of America, Washington, DC 20064.
E-mail: sheehan@cua.edu
Received June 17, 2002; Accepted October 19, 2002.
DOI 10.1002/jmri.10253
Published online in Wiley InterScience (www.interscience.wiley.com).

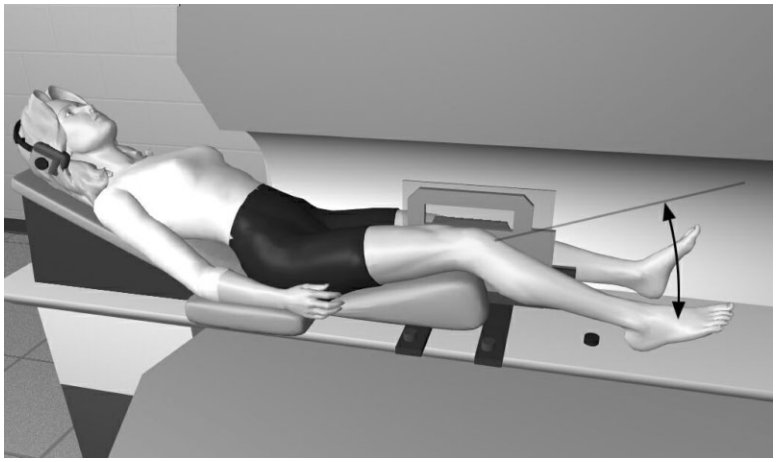

Figure 1. Volunteer position within the imager. A cushioned wedge, placed under the subject's thigh, was adjusted so that he or she could reach full knee extension. Cushions were used to support the neck and head and to raise the subjects' backs from the bed, reducing hip extension slightly. A previously designed coil holder (16) was adapted to stabilize two phased array cardiac coils on either side (medial/lateral) of the knee. An optical trigger was placed beneath the ankle and used to mark the beginning of the motion cycle. A metronome was played through the headphones to aid the subject in maintaining a motion rate of 35 cycles/minute.

angles throughout the motion cycle can be accomplished analytically. Other dynamic imaging methods calculate clinical angles by locating specific landmarks on anatomic images at every time frame during either movement or static positioning (11,18). This requires intensive operator intervention, resulting in possible inconsistencies in defining anatomical landmarks, whereas with VFA we can identify landmarks in a single image and then analytically track these landmarks based on the 3D kinematics (21).

The current study builds toward this ultimate goal by acquiring noninvasive and in vivo 3D dynamic joint data during an actively loaded functional movement with the expressed aim of quantifying precision. Similar to the previous work of Sheehan et al (16) and Sheehan and Drace (21), this study focuses specifically on the knee joint. Unlike previous kinematic cine MRI knee joint studies, we quantify the 3D kinematics of the complete knee (patello-femoral-tibial). Thus, the classic patellofemoral angles (e.g., patellar tilt angle and lateral patellar tilt) along with the knee angle can be quantified at every time frame and the latter does not have to be approximated (10).

MATERIALS AND METHODS

Eight healthy subjects (6 female, 2 male; age range = 33.0 ± 11.3 years; weight = 65.8 ± 12.4 kg; height = 168.4 ± 9.0 cm) participated in this Institutional Review Board-approved study. All subjects had no prior history of knee problems or pain and, upon physical examination, presented with normal knee appearance. Both knees of each subject were imaged. After obtaining informed consent, subjects were placed in a 1.5-T MR imager (CX; GE Medical Systems, Milwaukee, WI). A cushioned wedge, placed under the subject's thigh, was adjusted so that he or she could reach full knee extension (Fig. 1). The degree of knee flexion attained by subjects depended on the length of their lower leg, due to the fixed inner diameter of the imager. Cushions were used to support the neck and head and to raise the subjects' backs from the scanner bed, reducing hip extension and fatigue in the adductors during movement. A custom-designed coil holder (16) stabilized two phased array cardiac coils on either side (medial/lateral) of the knee. An optical trigger placed on the imaging bed, beneath the ankle, synchronized the data collection to the motion cycle.

For the dynamic imaging sequences, subjects were asked to cyclically extend and flex their knee at 35 cycles/minute to the beat of an auditory metronome (two beats/cycle). Prior to data collection subjects practiced the required task until they could do it comfortably and consistently. A single dynamic exam involved three movement trials. During the first trial, anatomic images were collected, using a cine gradient echo sequence, at the level of the femoral epicondyles (1 axial plane, 24 time frames, imaging time = 0:31 seconds). These images were used to select a sagittal or sagittal-oblique plane that was perpendicular to the femoral epicondyles and bisected the patella (Fig. 2a). At this single-slice location, a full cine-PC or fast-PC, which uses segmented phase encoding, data set was collected (anatomic and x, y, and z velocity images, 24 time frames, imaging times varied; Fig. 3). One of three possible sequences were chosen for this collection; each sequence had a field of view (FOV) of 30 × 22.5 cm (in-plane resolution = 1.17 × 1.17 mm), slice thickness of 10 mm, echo time of minimum full, flip angle of 30°, and maximum velocity encoding (v_{enc}) of 20 cm/second, and the data were sorted to 24 time frames. The three possible sequences used were:

1. Cine-PC2: cine-PC MR (time = 5:33), 2 acquisitions (data averaging), repetition time (TR) = 21 msec, temporal resolution = 84 msec
2. Cine-PC1: cine-PC MR (time = 2:49), 1 acquisition (no data averaging), TR = 21 msec, temporal resolution = 84 msec
3. Fast-PC2: fast-PC MR (time = 2:48), 2 acquisitions (data averaging), 2 phase encoding acquisitions, TR = 9 msec, temporal resolution = 72 msec

Finally, fast cine gradient echo anatomic images were collected at three axial levels defined at full extension (Fig. 2b): through the midpatella (measured superior to inferior), through the femoral epicondyles, and through the tibia, approximately 2 cm below the patellar tendon tibial insertion (time = 1:33, 1 acquisition, 8 phase encoding acquisitions, 24 time frames, TR = 7 msec, temporal resolution = 54 msec). Subjects rested a min-

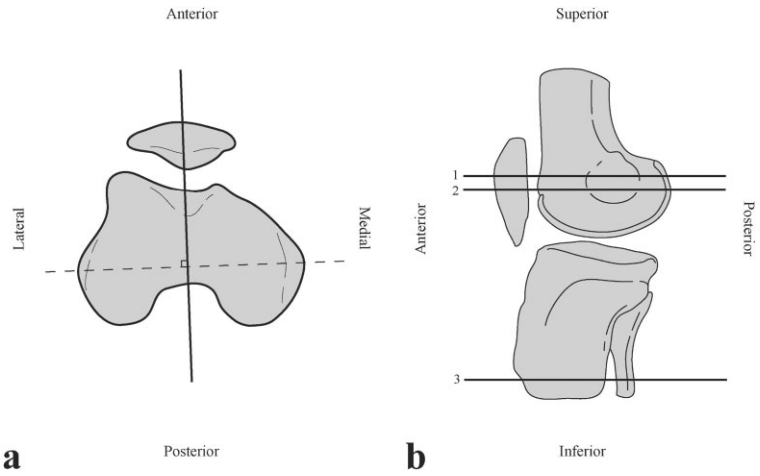

Figure 2. a: The PC sagittal or sagittal-oblique plane location was perpendicular to the femoral epicondyles bisecting the patella. **b:** Fast cine axial image plane location selected from the anatomic PC images when the leg was in full extension. The locations were through 1) the femoral epicondyles, 2) the midpatella, and 3) the tibia, approximately 2 cm below the patellar tendon tibial insertion.

imum of 2 minutes between trials. Subject compliance, bone size (i.e., the in-plane cross section of the bones was large enough for the analysis performed) and image clarity were the criteria used for accepting an image data set.

Rigid body translations and rotations of the femur, tibia and patella were quantified through analyses performed using the anatomic images and velocity data obtained during the dynamic exam. Regions of interest (ROIs), defined by a series of vertices, were graphically prescribed on each bone. The size of the ROIs ranged from 49–950 pixels based on the bone size and the type of analysis performed. Using a program developed by Zhu et al (20), the position and velocity of the ROI vertices were calculated for the entire motion cycle based on Fourier integration.

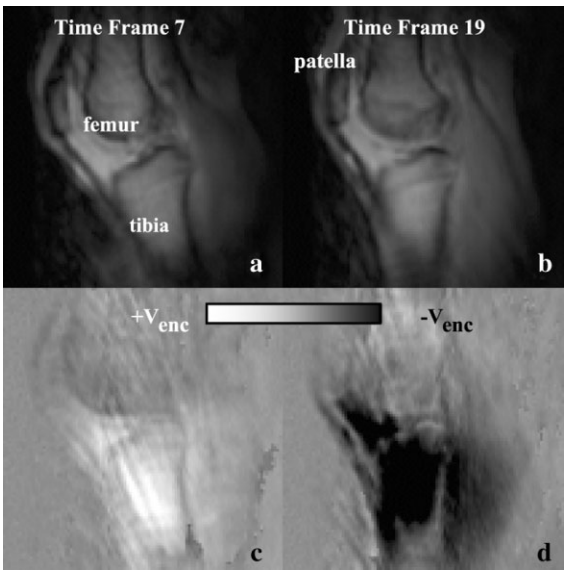

Figure 3. a and **b:** Sample cine-PC MR anatomic images. **c** and **d:** Velocity images are anterior/posterior (A/P) velocity images (superior/inferior and medial/lateral images not shown). White/black pixels indicate maximum A/P velocity. For example, the white pixels in (c) demonstrate the anterior tibial velocity during extension.

The orientation matrices describing the 3D orientation of each bone relative to the imager were determined from the displacement trajectories of the ROI vertices using rigid body mechanics. The initial bone orientation was calculated using anatomically based coordinate systems, defined using landmarks identified in the dynamic sagittal and axial anatomic images (16). These landmarks were identified in a single time frame only, when the knee was in full extension. Guidelines were established prior to the analysis in order to objectively define these landmarks. Through matrix multiplication, the orientation matrices for each bone relative to the imager were converted into the orientation matrices of the patella in reference to the femur (patellofemoral orientation) and of the tibia in reference to the femur (tibiofemoral orientation). For data presentation, the orientation matrices were simplified to orientation angles (Fig. 4) based on an xyz body-fixed rotation sequence (22,23).

The subject interexam variability (SIEV) was defined as the absolute difference in patellofemoral and tibiofemoral orientation between two exams for the same subject using the identical imaging protocol. To quantify SIEV, data were collected using one of three possible PC protocols: cine-PC2, cine-PC1, or fast-PC2. The subject then rested (minimum of 2 minutes) and the exam was repeated using the same protocol as the first exam. Both the protocol selected and the presentation order were randomly selected. We limited each SIEV test to only two dynamic exams in order to avoid subject fatigue. Due to subject time constraints, SIEV tests were completed for two of the three possible PC protocols on each knee.

The patellofemoral and tibiofemoral orientation angles were calculated by integrating the data from each SIEV exam. The ROIs used for these analyses were chosen to be as large as possible while remaining within the confines of the bone (Fig. 5a). In order to quantify the SIEV, each orientation angle (e.g., patellofemoral flexion, tilt, and twist; Fig. 4) was interpolated to 1° knee angle increments and the absolute difference for each orientation angle was calculated between the exams at each knee angle increment.

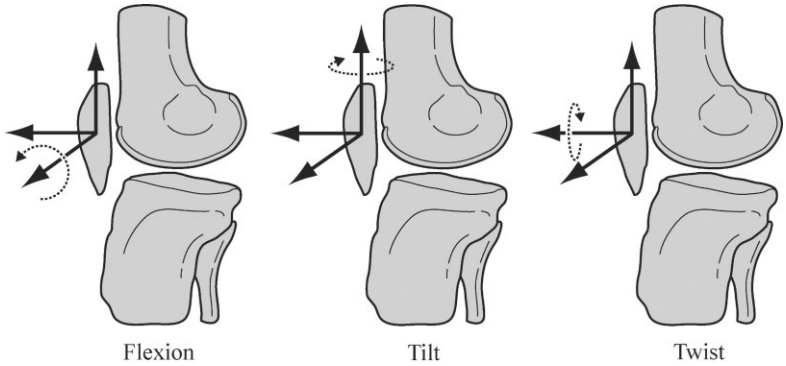

Figure 4. Patellar orientation angles (flexion, tilt, and twist). Such a mathematical interpretation describes the orientation of one body relative to another by assuming that the fixed coordinate systems in each body begin aligned. Then one body is brought into its final position by first rotating the body about the x-axis (flexion), then about the y-axis (tilt), and then about the z-axis (twist). This methodology produces angles of tibial flexion and patellar tilt that are nearly identical to those measured using classic clinical definitions of patellar tilt and knee flexion (21). Since these data were taken with respect to time and not knee flexion angle, interpolation was used to present the orientation angles with respect to knee angle in 1° knee angle increments (23).

The precision (the variance due to the inherent precision of each of the three above-listed protocols, separate from that due to SIEV) was defined as the standard deviation of the average orientation angles determined by 10 independent analyses of the same exam. These 10 analyses were obtained from 10 independent ROIs (49 pixels in each) on the femur and tibia from a single exam for each knee (Fig. 5b). The standard deviations of the average orientation angles, describing the tibial and femoral orientation relative to a fixed coordinate system, varied over time. Thus, the average precision over the 24 time frames is reported. Additionally, maintaining spatial independence of the ROIs required the use of artificially small regions (49 pixels) compared to those used in a typical exam (~900 pixels). Thus, the reported precision was scaled based on the inverse relationship of variance and the square root of the number of pixels contained within the ROI (24). The reported tibial and femoral precision was the average precision scaled by $\sqrt{49/920}$ and $\sqrt{49/900}$, respectively. These scaling factors were based on the fact that the average region for a standard exam is 920 pixels for the tibia and 900 pixels for the femur.

The precision was calculated for all three PC protocols on all knees. The data for two of the protocols were obtained from the first exam of each of the two SIEV tests. A fifth exam was performed after the two SIEV exams in order to obtain data for the third PC exam, the one for which a SIEV test was not performed due to time constraints. In total, all knees underwent five exams using three protocols. All exams were completed within a 3-hour period. The one exception was a single female subject who was able to complete three SIEV tests on both legs during the time allotted.

RESULTS

The average precision for all three PC imaging protocols ranged from 0.2°–1.2° (Table 1). As expected, due to the tibia's larger range of motion, the precision was better for the femur than for the tibia. Cine-PC2 had the best

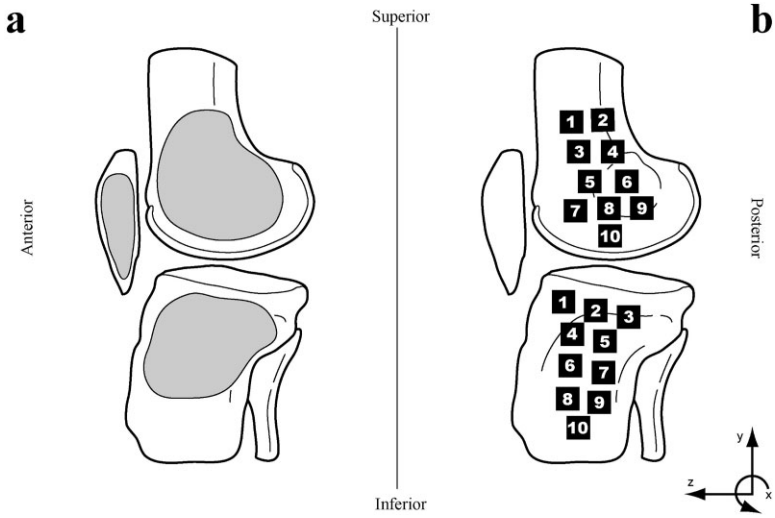

Figure 5. a: Placement of large regions for SIEV test. **b:** Placement of small regions used for calculating precision.

Table 1
Precision of all Phase Contrast Methods

11 Knees	Femur			Tibia		
	Tilt	Flexion	Twist	Tilt	Flexion	Twist
Fast-PC2	.29° ± .10	.45° ± .08	.22° ± .04	.55° ± .19	1.16° ± .23	.49° ± .09
Cine-PC2	.36° ± .10	.53° ± .07	.33° ± .10	.33° ± .10	.63° ± .17	.37° ± .10
Cine-PC1	.39° ± .06	.68° ± .08	.35° ± .06	.48° ± .12	.88° ± .18	.46° ± .07

precision when analyzing tibial data, whereas fast-PC2 had the best precision when analyzing the femoral data.

The results of this study demonstrate that subjects can produce repeatable knee joint kinematics (Table 2). The data trends were quite similar between both exams for most tests, but some were separated by a constant offset (Fig. 6). The SIEV was best for patellofemoral and tibiofemoral kinematics when using fast-PC2 compared to cine-PC1 and cine-PC2 (Table 2). The variances for patellofemoral and tibiofemoral kinematics range from 1.5°–2.7° and 0.8°–2.0°, respectively, when using fast-PC2. The SIEV for tibiofemoral kinematics was slightly better for most knees than that for patellofemoral kinematics.

DISCUSSION

The current study confirms that 3D skeletal kinematics can be quantified in a highly precise manner using PC MRI data. Acquiring 3D velocity data allows skeletal displacements and changes in orientation to be quantified without the need to visually identify numerous anatomical landmarks in every time frame. Instead, specific regions are identified on the bone (at t = 0) and tracked through the motion cycle using integration. Based on the principles of rigid body motion, these data can then be used to calculate the trajectory of any point on the bone (regardless of its initial location). This more objective MRI method not only reduces analysis time, but also reduces operator intervention, which should improve precision. Also, the three-dimensionality of these data gives us the ability to track clinical angles in multiple planes; therefore, we do not have to approximate out-of-plane angles, such as knee flexion angle, as was done in previous cine studies (18). Thus, this tool holds great potential for advancing clinical research in the area of joint function by allowing for accurate and precise quantified measures of musculoskeletal kinematics.

Three-dimensional joint kinematics, obtained with minimal or no subjective interpretation, are highly valuable to the clinician because they allow for a precise quantifiable definition of the joint impairment (1,25). This fosters the development of individualized treatment plans for specific impairments, which should produce improved outcomes for the patient. Specifically, the starting point of any intervention for joint impairments must be to accurately quantify the 3D joint kinematics. In addition, defining alterations in joint kinematics due to intervention requires not only that we understand the variability within healthy and specific patient populations, but also that we know the variability within individual subjects.

One possible limitation of the current study is that the accuracy of the fast-PC2 technique was not tested. Due to numerous methodology refinements the accuracy of the fast-PC2 technique should be equal to or better than the accuracy measured previously for cine-PC MRI (2). We have improved the velocity resolution, temporal resolution, and the signal-to-noise ratio (SNR). We were able to improve the velocity resolution by dropping the velocity encoding (v_{enc}) from 35 to 20 cm/second (a 57% improvement) without aliasing. Also, the areas of the ROIs analyzed in the phantom study were limited due to its design. When analyzing in vivo skeletal motion, these regions can be much larger, improving SNRs and decreasing variance (24). Lastly, the temporal resolution of fast-PC is 14% (84 vs. 72 msec) better than that of cine-PC MRI due to a decrease in the TR. Note: This represents an improvement in temporal resolution over previous cine joint studies as well. For example, Brossmann et al (26) used an approximate temporal resolution of 190 msec. It is difficult to compare the accuracies of our measures with previous cine kinematic studies because these measures have not been explicitly stated (18,26). Yet, the accuracy of previous cine MRI knee joint kinematics studies is pixel size limited. Thus, the highest expected accuracy would be on the order of 1.55 mm.

Precision is typically defined as the variation in the output (standard deviation or standard error) from repeated measures of the identical experiment. Due to subject fatigue and SIEV, we could not perform identical repeated exams for each protocol numerous times (e.g., 10). Thus, in order to quantify precision we analyzed 10 independent regions on the femur and tibia

Table 2
Subject Inter Exam Variability (SIEV) for Patellofemoral and Tibiofemoral Kinematics

	No. knees	Patellofemoral			Tibiofemoral		
		Tilt	Flexion	Twist	Tilt	Flexion	Twist
Fast-PC2	7	2.4°	1.6°	2.3°	1.4°	2.0°	0.8°
Cine-PC2	7	6.1°	2.4°	3.1°	1.9°	2.8°	1.6°
Cine-PC1	6	3.6°	2.3°	4.7°	1.5°	3.5°	1.3°

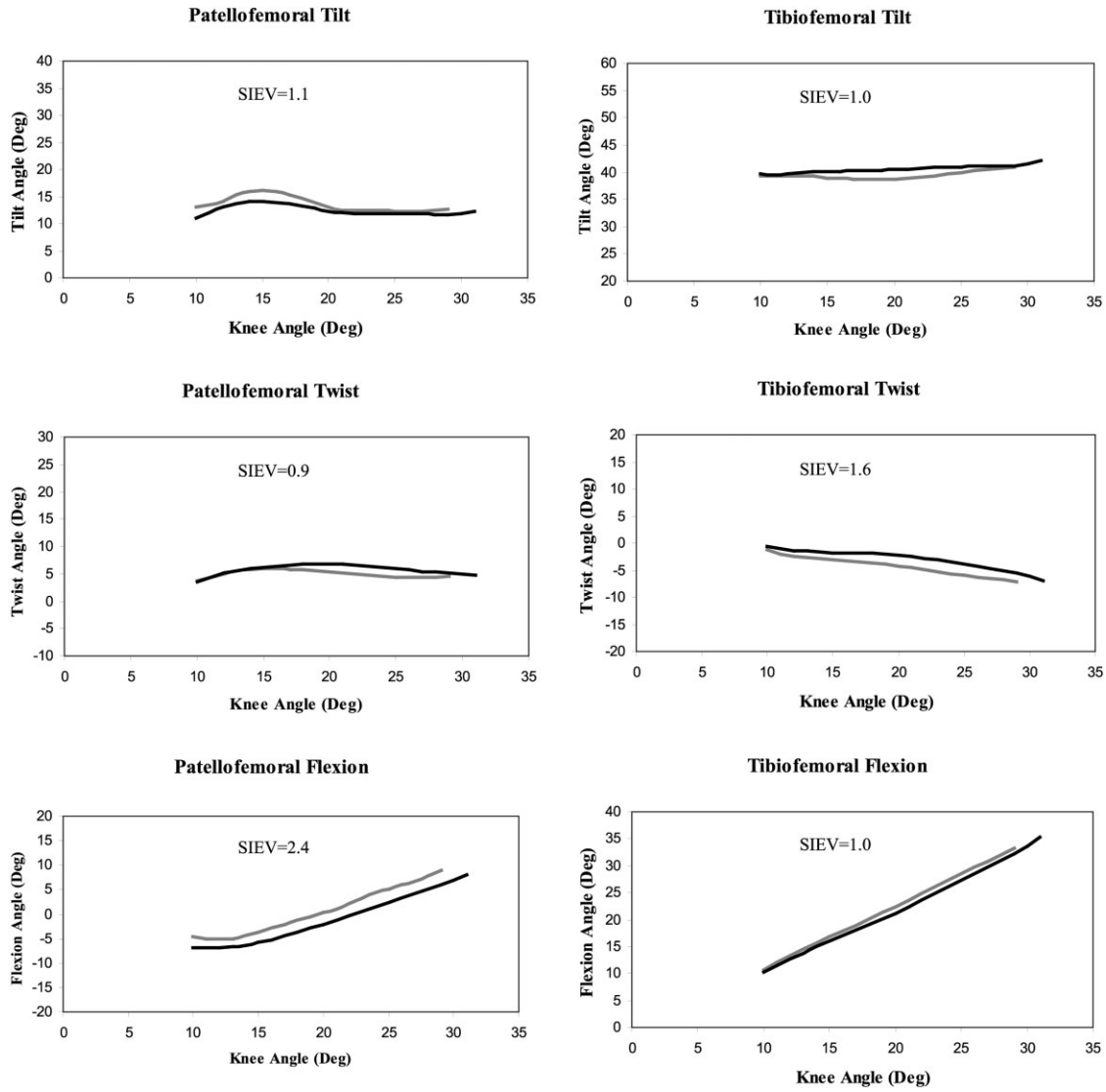

Figure 6. Repeatability plots. These graphs represent the SIEV of orientation angles (tilt, twist, and flexion) for patellofemoral and tibiofemoral kinematics for a single volunteer. The black line represents trial 1, and the gray line represents trial 2. All plots have a 40° range in the y-axis and a 35° range in the x-axis.

from a single exam for each knee. The patella was excluded from this study because 10 independent regions could not be prescribed on this small bone. In order to define 10 spatially independent regions within the confines of each bone, the regions were artificially small (49 pixels). Since the predicted variance in the estimated displacement measures (24) is inversely proportional to the number of pixels within the region analyzed, the calculated precision was scaled by the square root of the number of pixels used in a standard knee joint exam (~900 pixels) divided by the number of pixels used in the current exam (49 pixels). Thus, based purely on the precision of fast-PC2, differences in knee joint kinematics in the range of 0.2°–1.2° should be distinguishable.

Comparison of the precision for all three techniques indicates that fast-PC2 and cine-PC2 have the best precision when analyzing tibial and femoral kinematics, respectively. The differences in precision between the two protocols are most likely dependent upon the presence of motion artifacts within the data and the susceptibility of the individual imaging protocol to these artifacts. Since fast-PC MRI collects data at greater than twice the rate (shorter TR) than cine-PC MRI (31.2 vs. 16.0 kHz), it can collect two phase encodes per cycle instead of a single phase encode, as is done with cine-PC. Thus, the imaging time can be halved without a loss of temporal resolution. A slight loss in SNR does occur because of the shorter TR, making fast-PC MRI more susceptible to motion artifacts than cine-PC MRI. On the flip side, the shorter imaging time reduces SIEV.

A primary limitation in all MRI, but particularly in dynamic MRI, is that motion artifacts can deteriorate the data to such a point that they become unusable. These artifacts are primarily due to inconsistent move-

ment and pulsatile motion within the imaging plane. In our studies, consistency of motion is controlled by giving subjects ample practice time and by providing a metronome to guide their movements. In studying the knee joint, the popliteal artery is a potential source of large artifacts. This is particularly problematic if these artifacts overlay the patella, due to the small size of this bone. Selecting a sagittal or sagittal-oblique imaging plane that was at least 5 mm distant from the popliteal artery eliminated these artifacts from overlaying the patella, but the artery was within the imaging plane at the level of the tibia for a single exam and contaminated these data.

Comparing joint kinematics across populations or following changes in joint function due to intervention should be much improved using this methodology, which is based on anatomically based coordinate systems and quantitative data analysis. Direct comparison of the precision and SIEV of the PC techniques examined in the current study to other imaging techniques is difficult because such measures have not been consistently reported previously. When deriving joint kinematics from PC data, anatomical landmarks are defined once for each individual exam and analytically tracked throughout the whole motion cycle. Thus, the potential for investigator bias is greatly reduced. Our process of identifying anatomical landmarks is not yet fully automated; thus, some investigator bias is possible, resulting in some small variation in landmark definition. Other imaging studies using CT (8,9) and MRI (11) acquire 2D data in the axial plane either statically or dynamically and estimate the 3D patellofemoral kinematics using 2D clinical measures (e.g., lateral patellofemoral angle (LPA)). Since these studies only acquire 2D data, the knee angle can only be estimated, not measured. Having an independent measure of knee angle should enhance the precision of our data.

Knowledge of SIEV is critical to define changes in joint kinematics after an intervention. Without such measures it is difficult to determine if observed changes in joint kinematics over time (26) are truly due to the intervention or are merely inherent variability within an individual or measurement technique. Subject variability using cine-PC1 was quite high, although it had comparable precision to both cine-PC2 and fast-PC2. Cine-PC1 and fast-PC2 have equal imaging times, but since data averaging is not used in cine-PC1 the SNR is reduced by 0.707 times as compared to cine-PC2. Based on our results it can be seen that most of the variability within and between exams is not related to technique precision, but to subject factors and the precision of the coordinate system definition. Thus, further improvements in SIEV and precision will be achieved from decreased scan times.

Through these studies we found that fast-PC2 has comparable precision, but improved SIEV compared to cine-PC2. In addition, fast-PC2 has shorter imaging times, which increases exam tolerance, particularly for patients with joint impairments. When expanding this protocol to study specific pathologies patients may not be able to perform prolonged movement studies, due to pain and fatigue. For such cases, the shorter time of fast-PC2 becomes a critical factor. Specifically, Brossmann et al (26) did not report fatigue or pain problems when they included patellar maltracking patients within a study requiring 2 minutes 13 seconds of movement, which is similar to the required time for fast-PC2. Thus, the use of fast-PC2 has clear clinical advantages over previous cine-PC and cine MRI methodology under these conditions.

ACKNOWLEDGMENTS

The authors acknowledge the Physical Disabilities Branch and Diagnostic Radiology Department of the National Institutes of Health for offering their resources. Additionally, the authors thank Jere McLucas for his help with the illustrations; Nao Shibanuma, Tracy Rausch, and Hany Bedair for their aid in data collection; and Dr. Steven Stanhope and Dr. Larry Yao for their insights into manuscript revision. We also thank Dr. Peter Choyke and Sandra Jones for their support in this project.

REFERENCES

1. Grelsamer RP. Patellar malalignment. J Bone Joint Surg Am 2000; 82A:1639–1650.
2. Sheehan FT, Zajac FE, Drace JE. Using cine phase contrast magnetic resonance imaging to non-invasively study in vivo knee dynamics. J Biomech 1998;31:21–26.
3. Drace JE, Pelc NJ. Tracking the motion of skeletal muscle with velocity-encoded MR imaging. J Magn Reson Imaging 1994;4:773–778.
4. Grabiner MD, Koh TJ, Draganich LF. Neuromechanics of the patellofemoral joint. Med Sci Sports Exerc 1994;26:10–21.
5. Laurin CA, Dussault R, Levesque HP. The tangential x-ray investigation of the patellofemoral joint: x-ray technique, diagnostic criteria and their interpretation. Clin Orthop 1979;144:16–26.
6. Merchant AC, Mercer RL, Jacobsen RH, Cool CR. Roentgenographic analysis of patellofemoral congruence. J Bone Joint Surg Am 1974; 56:1391–1396.
7. Nietosvaara AY, Aalto KA. Ultrasonographic evaluation of patellar tracking in children. Clin Orthop 1993;297:62–64.
8. Dupuy DE, Hangen DH, Zachazewski JE, Boland AL, Palmer W. Kinematic CT of the patellofemoral joint. AJR Am J Roentgenol 1997;169:211–215.
9. Schutzer SF, Ramsby GR, Fulkerson JP. The evaluation of patellofemoral pain using computerized tomography. A preliminary study. Clin Orthop 1986;3:286–293.
10. Powers CM, Shellock FG, Pfaff M. Quantification of patellar tracking using kinematic MRI. J Magn Reson Imaging 1998;8: 724–732.
11. Brossmann J, Muhle C, Schroder C, Melchert UH, Bull CC, Spielmann RP, Heller M. Patellar tracking patterns during active and passive knee extension: evaluation with motion-triggered cine MR imaging. Radiology 1993;187:205–212.
12. Grabiner MD, Koh TJ, Miller GF. Fatigue rates of vastus medialis oblique and vastus lateralis during static and dynamic knee extension. J Orthop Res 1991;9:391–397.
13. Heegaard J, Leyvraz PF, Van Kampen A, Rakotomanana L, Rubin PJ, Blankevoort L. Influence of soft structures on patellar three-dimensional tracking. Clin Orthop 1994;299:235–243.
14. Lafortune MA, Cavanagh PR, Sommer III HJ, Kalenak A. Three-dimensional kinematics of the human knee during walking. J Biomech 1992;25:347–357.
15. Veress SA, Lippert FG, Hou MC, Takamoto T. Patellar tracking patterns measurement by analytical x-ray photogrammetry. J Biomech 1979;12:639–650.
16. Sheehan FT, Zajac FE, Drace JE. In vivo tracking of the human patella using cine phase contrast magnetic resonance imaging. J Biomech Eng 1999;121:650–656.

17. Muhle C, Brossmann J, Heller M. Kinematic CT and MR imaging of the patellofemoral joint. Eur Radiol 1999;9:508–518.
18. Shellock FG, Stone KR, Crues JV. Development and clinical application of kinematic MRI of the patellofemoral joint using an extremity MR system. Med Sci Sports Exerc 1999;31:788–791.
19. Hughston JC, Deese M. Medial subluxation of the patella as a complication of lateral retinacular release. Am J Sports Med 1988; 16:383–388.
20. Zhu Y, Drangova M, Pelc NJ. Fourier tracking of myocardial motion using cine-PC data. Magn Reson Med 1996;35:471–480.
21. Sheehan FT, Drace JE. Quantitative MR measures of three-dimensional patellar kinematics as a research and diagnostic tool. Med Sci Sports Exerc 1999;31:1399–1405.
22. Kane TR, Likins PW, Levinson DA. Spacecraft dynamics. New York: McGraw-Hill, 1983. p 20–23.
23. Sheehan FT, Mitiguy P. In regards to the "ISB recommendations for standardization in the reporting of kinematic data." J Biomech 1999;32:1135–1136.
24. Pelc NJ, Sommer FG, Li KC, Brosnan TJ, Herfkens RJ, Enzmann DR. Quantitative magnetic resonance flow imaging. Magn Reson Q 1994;10:125–147.
25. Witonski D, Goraj B. Patellar motion analyzed by kinematic and dynamic axial magnetic resonance imaging in patients with anterior knee pain syndrome. Arch Orthop Trauma Surg 1999;119:46–49.
26. Brossmann J, Muhle C, Bull CC, Zieplies J, Melchert UH, Brinkmann G, Schroder C, Heller M. Cine MR imaging before and after realignment surgery for patellar maltracking—comparison with axial radiographs. Skeletal Radiol 1995;24:191–196.